

MICROWAVE CHARACTERIZATION OF BIO-COMPOSITES MATERIALS BASED FINITE ELEMENT AND NICHOLSON-ROSS-WEIR METHODS

Ahmad F. Ahmad^{1*}, Zulkifly Abbas^{1,2}, Suzan J. Obaiys², Norazowa Ibrahim³, M.F. Zainuddin⁴

¹Institute for Mathematical Research, Universiti Putra Malaysia Serdang, Selangor Darul Ehsan, Malaysia.

²Department of Physics, Faculty of Science, Universiti Putra Malaysia, Serdang, Selangor Darul Ehsan, Malaysia.

³Chemistry Department, Faculty of Science, Universiti Putra Malaysia, Serdang, Selangor Darul Ehsan, Malaysia.

⁴Environmental Sciences Department, Faculty of Environmental Studies, Universiti Putra Malaysia, Serdang, Malaysia.

*Corresponding Author: ahmad_al67@yahoo.com

ABSTRACT In this work, Bio-composite of oil palm empty fruit bunch fibre (OPEFB)-filler and polycaprolactone (PCL)-polymer has been prepared and characterized. The functional groups and morphology of the prepared samples were characterized by Fourier transform infrared spectroscopy (FT-IR). By using the Nicholson-Ross-Weir (NRW) mode, both of real and imaginary relative permittivity values of the samples were obtained simultaneously from the reflection and transmission coefficient measurements of the materials. Whereas, the attenuation with the field distribution at the waveguide filled with a sample were considered by using the Finite Element Method (FEM). The magnitude of the reflection and transmission (R/T) coefficients of the composite with different filler percentages were measured using rectangular waveguide in conjunction with a microwave vector network analyzer (VNA) in X-band range of frequency. The computations of the S-parameters were achieved by using the FEM technique along with NRW mode. Then, the obtained results were compared with the measured R/T coefficients. Relative error results nominated the FEM mode due to its highly accurate results than the other method.

(Keywords: Microwave measurements, OPEFB, PCL, Bio-composite)

INTRODUCTION

Fibres are generally added to commercial matrix resins to modify properties such as stiffness, tensile strength, heat distortion and mold ability [1]. The level of enhancement depends mainly on the type of filler, size, shape, fibre loading, and surface treatment which supports interaction between the filler and the polymer [2]. Several past studies suggested that natural fibre-based composites show remarkably outstanding performances and can be produced with a large volume at affordable costs [3, 4]. OPEFB fibre has received increased attention since it is inexpensive to obtain, biodegradable, non-toxic and available in great quantity [5,6]. Several studies supported the incorporation of OPEFB fibre into different types of polymer matrices to obtain cost reduction and reinforcement [7]. The properties of thermoplastic composites are generally influenced by the processing parameters such as a mixing time, rotor speed (rpm), and temperature in the compounding process [8]. The melt-mixing method is more advantageous due to its simplicity and cost effectiveness over other methods such as solution mixing which is more expensive and time consuming [9,10]. Several approaches have been proposed to obtain the electromagnetic properties of reflection and transmission coefficients for the samples [11,12]. The

transmission reflection rectangular waveguide technique (T/R) was conducted in order to obtain the reflection and transmission coefficients of the materials [13].

This study reports the morphological properties of the OPEFB-PCL composites by using Thermo gravimetric and spectroscopy analysis FT-IR. In addition, COMSOL software was utilized based on the FEM to approximate the rectangular waveguide of three-dimensional geometry, where the model consists of a rectangular waveguide with microwave propagation transition through it. For the wave propagation problem, the RF Module's Port boundary condition was enforced in this model. The FEM mode implemented the boundary condition to determine the distribution of the electric field intensity. Thus, the computation of the electromagnetic properties of reflection and transmission coefficients was accomplished based on the fundamental components of both FEM and NRW theorems. A comparable performance of the obtained theory results to the measured reflection and transmission coefficient values were discussed at microwave frequency. The VNA was calibrated by using the standard two-port calibration mechanism (SOLT).

THEORY

Finite Element Method (FEM)

In this paper, FEM mode was implemented for the determination of the S-Parameters of OPEFB-PCL composites that was loaded in a rectangular waveguide which was divided into three main regions (I, II and III) for the analysis requirement. For the step formulations, the electric field in the rectangular waveguide was discretized based tetrahedron elements Fig. 1.

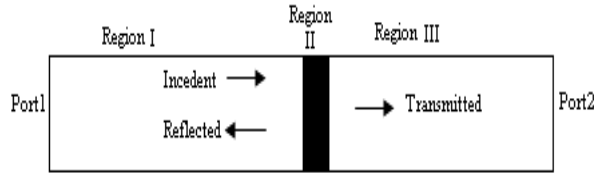


Figure 1. Incident transmitted and reflected electromagnetic waves in a filled transmission line.

In each tetrahedron, the unknown field can be interpolated from each node value by using the first order polynomial of the form [14]

$$\rho^e(x, y, z) = a^e + b^e x + c^e y + d^e z \quad (1)$$

While, the electric field E can be calculated from

$$E^e = \sum_{i=1}^6 N_i^e E_i^e(x, y, z) \quad (2)$$

Where $N_i^e; i = 1, 2, 3...6$ are the six complex amplitudes of E associated with the six edges of the tetrahedron, and $E_i^e(x, y, z)$ is the vector basis function associated with the i^{th} edge of the tetrahedron. The global matrix equation over all the tetrahedron elements in the sample region can be given as follow

$$[S] \times \{N_i\} = \{v\} \quad (3)$$

The vector solution $\{N_i\}$ of the matrix equation in (3) is then applied for the determination of the reflection (R) and transmission (T) coefficients which are defined as follow

$$R = \iint_{\text{over } S_1} \vec{E} \times \vec{e}_0 ds - 1 \quad (4)$$

$$T = \iint_{\text{over } S_2} \vec{E} \times \vec{e}_0 ds \quad (5)$$

Where, COMSOL software utilized the values of R and T in (4) and (5) respectively.

Nicolson-Ross-Weir algorithm

Nicholson-Ross-Weir (NRW) theorem [15] provided a direct calculation of both the permittivity and permeability from the input S-parameters. It is the most commonly used technique for performing such conversions where the measurement of reflection (R) and transmission (T) coefficients require both values of S-parameters for the material under test to be measured. The reflection coefficient equation is given by

$$R = X \pm \sqrt{X^2 - 1} \quad (6)$$

Where

$$X = \frac{(S_{11}^2 - S_{21}^2) + 1}{2S_{11}} \quad (7)$$

While T is given by

$$T = \frac{(S_{11} - S_{21}) - R}{1 - R(S_{11} + S_{21})} \quad (8)$$

EXPERIMENTAL SECTION

Sample Preparation

The mixing process of OPEFB-PCL compound was accomplished in a Thermo Haake machine by blending the fibre of 250µm size and PCL polymer at 70°C with rotor speed at 50 rpm for only 20 minutes. The substrates were prepared by placing 10 g of the blends into a mold of 10-8cm² dimensions and 1 mm thickness. After that, OPEFB-PCL compounds were preheated for 10 minutes with the top and bottom plate in 70°C. A 10 second breathing time was allowed for bubble sand releasing to reduce the void and then pressed at the same temperature for another 10 minutes with 110 kg/cm² pressure. Finally, a cooling with pressure 110 kg/cm² was carried out for another 10 minutes.

FT-IR spectroscopy

The FT-IR spectroscopy analysis was achieved by using a Spectrum 100, FT-IR spectrometer, Perkin Elmer. For the testing case, a small sample was pressed into a film form and then analyzed. The transmission of infrared spectra was obtained in between pictorial representation 400 and 4000 cm⁻¹ ranges at the room temperature.

Dielectric and scattering parameter

The measurement of the dielectric properties of the material was performed with the industrial de-facto standard Agilent 85070E open ended coaxial dielectric probe kit. The measurement setup of S-parameters requires an Agilent N5230A PNA-L network analyzer and a pair of standard rectangular waveguide.

RESULTS AND DISCUSSION

FT-IR analysis was used to investigate the interaction of fillers onto PCL matrix and to verify the formation of ester bonds at the material interfaces. Fig. 2 shows the FT-IR spectra of OPEFB-PCL composites at room temperature with several specific stretching regions. It can be observed from the figure that there are strong and complex multiple peaks of carbon-oxygen (-O-C-O) stretching absorption between 1000 and 1300 cm⁻¹. Close inspection of the results reveal that these peaks do not significantly shift with the addition of OPEFB fibre in the composite. This implies that there is no extra interaction or new bond formed due to the mixing which is expected since the mixture of PCL and fibre are not chemically treated. Hence, the interaction between PCL and fibre is mainly due to chain entanglement of fibre particles-polymer matrix which improves the electrical and physical properties of the composites.

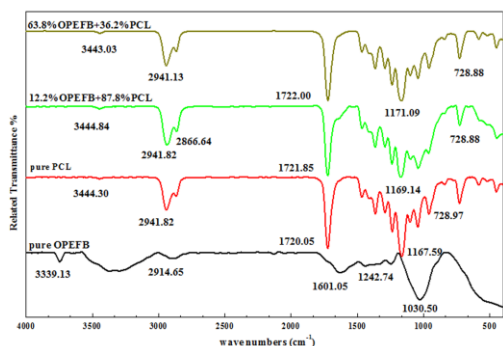


Figure 2. FT-IR spectra of the OPEFB-PCL composites.

Furthermore, the variation in dielectric constant (ϵ') and loss factor (ϵ'') of OPEFB fibre, PCL and the composite from 8 GHz to 12 GHz are shown in Fig. 3. Interestingly, it can be observed that the dielectric constant and loss factor of the OPEFB fibre, PCL and the composites are almost consistent in the X-band frequency.

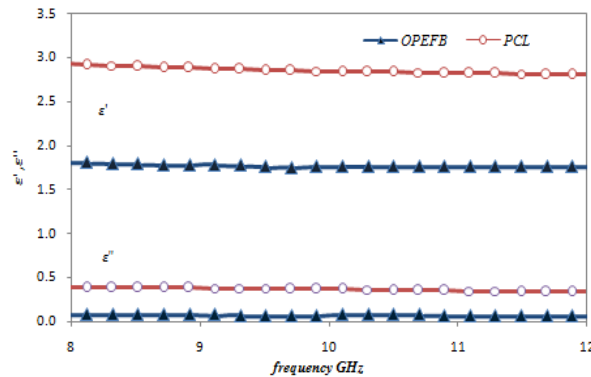


Figure 3. Dielectric constant (ϵ') and loss factor (ϵ'') of the OPEFB fibre and PCL polymer.

Comparison of the Measured and Calculated S-parameters

The comparisons between the calculated S-parameters, S₁₁ and S₂₁ based NRW formulations (6 to 8), FEM Method to the measurements are illustrated in the Fig. 4 and Fig. 5. The dielectric properties, which obtained from the measurement of OPEFB-PCL samples, were used as initial inputs to NRW and FEM to calculate the S₁₁ and S₂₁ of the composites. It is known that the convergence analysis was only carried out for FEM, while it is not required for the NRW formulations. Generally, in this figures, the magnitude of S₁₁ decreased and S₂₁ increased with the percentage increment of the OPEFB filler.

The higher value of the dielectric constant, the higher is the impedance mismatched at the surface of the sample inside the T/R rectangular waveguide. However, the materials with higher loss factor absorbed more energy.

The accuracy of S₁₁ and S₂₁ values can be decided through the relative error calculation with respect to the measurement results, as follows

$$\text{Relative error of } S_{11} = \frac{S_{11}(\text{measurement}) - S_{11}(\text{NRW, FEM})}{S_{11}(\text{measurement})} \quad (9)$$

The relative error of S_{11} and S_{21} from Table 1, shows that among the two applied methods, FEM is more accurate method than NRW when samples of OPEFB-PCL composite were tested. The mean relative error values of FEM were observed to be 0.287 and 0.048 respectively, while the value for NRW is reported as 0.460 and 0.096 respectively. Therefore, the FEM is recommended for this test. In spite of the NRW is based

on closed form, the numerical simulation showed better agreement. This is because of the calculation of the S-parameters using NRW involves several approximations that are mostly eliminated with the numerical simulation setup when samples of fibre reinforced polymer were tested for different percentage of OPEF filler.

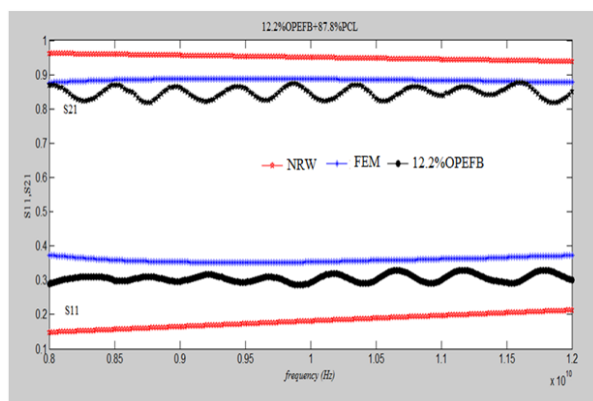


Figure 4. Comparison of measured, simulated and calculated S- Parameters (S_{11} , S_{21}) for 12.2% OPEFB + 87.8%PCL composites.

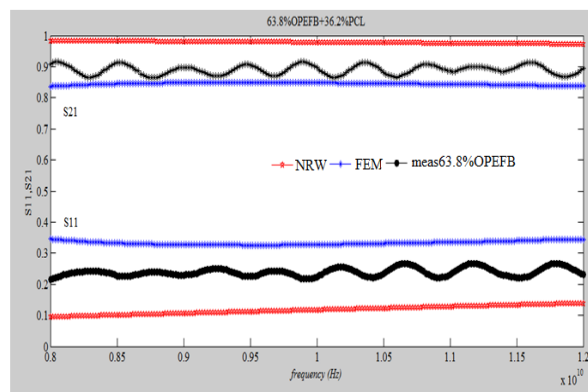


Figure 5. Comparison of measured, simulated and calculated S- Parameters S_{11} and S_{21} for 63.8% OPEFB + 36.2%PCL composites.

Table 1. Relative error of S_{11} and S_{21} for FEM and NRW of OPEFB-PCL composites

Sample	Mean Measured S-Parameters		Mean relative error			
	S_{11}	S_{21}	S_{11}		S_{21}	
			NRW	FEM	NRW	FEM
12.2%OPEFB +87.8%PCL	0.238	0.847	0.411	0.175	0.104	0.032
63.8%OPEFB +36.2%PCL	0.306	0.883	0.509	0.399	0.087	0.064
Mean Relative Error			0.460	0.287	0.096	0.048

CONCLUSION

In this work, OPEFB-PCL composites were successfully prepared by melt blending method. The FEM and NRW procedures have been presented to determine the distribution of electric field intensity of 1 mm thick composite. Where, the dielectric properties ($|S_{11}|$ and $|S_{21}|$) of the composite were obtained successfully by FEM, NRW and experimental method as well. Microwave properties of the composites were characterized using FT-IR spectroscopy which reveals any extra interaction or new bond formed due to the

mixing. It is clear that the composite of 12.2% filler exhibits higher $|S_{11}|$ and lower $|S_{21}|$ than the composite with the 63.5% filler. Generally, the given figures clearly marked the level of transmission is greater than reflection and the reflection and transmission coefficients that obtained by FEM technique are more accurate than the obtained NRW results based on the mean relative error values.

ACKNOWLEDGMENT

The first author is grateful for the research support through the Graduate Research Fellowship (IGRF) grant provided by University Putra Malaysia (UPM).

REFERENCE

1. Unal H. (2004). Morphology and mechanical properties of composites based on polyamide 6 and mineral additives. *Materials and Design*, Vol. 25, 483-487.
2. Dikobe D.G., Luyt A.S. (2009). Morphology and properties of polypropylene/ethylene vinyl acetate copolymer/wood powder blend composites. *eXPRESS Polymer Letters*, 3, 190-199.
3. Satyanarayana K.G., Sukumaran K., Mukherjee P.S., Pavithran C., Pillai, S.G.K. (1990). Natural fibre-polymer composites. *Cement and Concrete Composites*, 12 (2), 117-136.
4. Ku H., Wang H. Pattarachaiyakoop N.M., Trada M. (2011). A review on the tensile properties of natural fibre reinforced polymer composites. *Compos. Part B Eng.* 42 (4), 856-873.
5. Rozman H.D., Tay G.S. Abubakar A., Kumar R.N. (2001). Tensile properties of oil palm empty fruit bunch-polyurethane composites. *European Polymer Journal*, 37, 1759-1765.
6. Sreekala M.S., Kumaran M.G., Thomas S. (1997). Oil palm fibres: Morphology, chemical composition, surface modification, and mechanical properties. *Journal of Applied Polymer Science*, 66, 821-835.
7. González Alriols M., Tejado A., Blanco M., Mondragon I., Labidi J. (2009). Agricultural palm oil tree residues as raw material for cellulose, lignin and hemicelluloses production by ethylene glycol pulping process. *Chemical Engineering Journal*, 148, 106-114.
8. Joseph K., Filho R.D.T., James B., Thomas S., De Carvalho L.H. (1999). A review on sisal fibre reinforced polymer composites. *Revista Brasileira de Engenharia Agrícola e Ambiental*, 3, 367-379.
9. Chul Chun B., Cho T.K, Chong M.H., Chung Y.C., Chen J., Martin D., Cieslinski R.C. (2007). Mechanical properties of polyurethane/montmorillonite nanocomposite prepared by melt mixing. *Journal of Applied Polymer Science*, 106, 712-721.
10. Lin R.H., Liu Y.H., Chen Y.H., Lee A.C., Ho T.H. (2007). Morphology controls of the melt blending in a novel highly cross linked bismaleimide system. *European Polymer Journal*, 43, 4197-4209.
11. Baker-Jarvis and Dielectric J. Magnetic measurement methods in transmission lines: An overview. *Proceedings of the 1992 AMTA Workshop*, Chicago, Illinois. (1992).
12. Şimşek S., Işık C., Topuz E., and Esen B. (2006). Determination of the complex permittivity of materials with transmission/reflection measurements in rectangular waveguides. *AEU-International Journal of Electronics and Communications*, 60(9), 677-680.
13. Pathania D., Singh D. (2009). A review on electrical properties of fibre reinforced polymer composite. *International Journal of Theoretical and Applied Sciences*, 1(2), 34-37.
14. Soleimani H. et al. (2014). Electromagnetic properties of lanthanum iron garnet filled PVDF-polymer composite at microwave frequencies using finite element method (FEM) and Nicholson–Ross–Weir (NRW) method. *Digest J. of Nanomaterials & Biostructures*, 9, p. 53– 60.
15. Nicholson and. Ross G.F. (1970). Measurement of the Intrinsic Properties of Materials by time-Domain Technique. *IEEE Trans. Instr. Meas*, 19, p. 377-382.